

## Modeling long-term dynamics of crop evapotranspiration using deep learning in a semi-arid environment



Ahmed Elbeltagi<sup>a,b</sup>, Jinsong Deng<sup>a,\*</sup>, Ke Wang<sup>a</sup>, Anurag Malik<sup>c</sup>, Saman Maroufpoor<sup>d</sup>

<sup>a</sup> College of Environmental and Resource Sciences, Zhejiang University, Hangzhou, 310058, China

<sup>b</sup> Agricultural Engineering Dept., Faculty of Agriculture, Mansoura University, Mansoura, 35516, Egypt

<sup>c</sup> Punjab Agricultural University, Regional Research Station, Bathinda, 151001, Punjab, India

<sup>d</sup> Irrigation and Reclamation Engineering Dept., University of Tehran, Tehran, Iran

### ARTICLE INFO

**Keywords:**

Crop evapotranspiration  
DNN model  
Climate change  
Future projection

### ABSTRACT

Crop evapotranspiration ( $ET_c$ ) is one of the most basic components of the hydrologic cycle that is effective in irrigation system design and management, water resources planning and scheduling, and hydrologic water balance. Thus, precise estimation of  $ET_c$  is valuable for various applications of agricultural water engineering, especially in developing countries such as Egypt, which has lack of meteorological data, high cost and time to calculate  $ET_c$ , and lack of information on future  $ET_c$  values to consider management scenarios and increase production potential. Also, due to the existence of different climates in Egypt, the estimate of  $ET_c$  has become a challenge. To this end, the aim of this study was to estimate the  $ET_c$  to eliminate the limitations mentioned, and analyze the long-term dynamics of  $ET_c$  based on limited climate data and simple method. Three Egyptian governorates namely Ad Daqahliyah, Ash Sharqiyah, and Kafr ash Shaykh of Nile Delta, were selected as major wheat-producing sites. The required historical required climatic data were collected from open access data library while future data were from two extreme scenarios of the Representative Concentration Pathways (RCP) i.e., RCP 4.5, and RCP 8.5. The available dataset was divided into three parts: (i) calibration from 1970–2000, (ii) validation from 2000–2017, and (iii) prediction from 2022–2035. The deep neural network (DNN) was employed for incorporating historical data and predicting future  $ET_c$ . For the evaluation of generated DNN models, the research finding indicates that the correlation coefficients between actual versus predicted monthly  $ET_c$  were found to be 0.95, 0.96, and 0.97 for calibration period, and 0.94, 0.95 and 0.95 for validation at Ad Daqahliyah, Kafr ash Shaykh, and Ash Sharqiyah regions, respectively. For the simulation of future climatic data, maximum temperature ( $T_{max}$ ) will increased by 5.19 %, 4.22 %, and 20.82 %, minimum temperature ( $T_{min}$ ) will increased by 1.62 %, 36.44 %, and 27.80 %, and solar radiation (SR) will increased by 6.53 %, 18.74 %, and 28.83 % for the study locations, respectively. Moreover, the DNN model exposed that the Kafr ash Shaykh attain the highest values of  $ET_c$  with an increase of 11.31 %, slightly increased of 1.38 % for Ad Daqahliyah, and decreased by 15.09 % for Ash Sharqiyah in comparison to the historical data. Thus, the proposed model of crop water-use prediction effectively estimated  $ET_c$  of wheat and make an efficient decision. The developed models produced satisfactory results for water managers to save water and achieve the sustainability of agricultural water.

### 1. Introduction

Agricultural water resources in the context of changing climate conditions are decreasing in different regions of worldwide with more emphasis in the semi-arid and arid zones. Therefore, accurate evaluation of irrigation water needs for crops is an urgent to increase the productivity and efficiency of irrigation water-use (Farg et al., 2012). In addition, crop evapotranspiration ( $ET_c$ ) estimates are needed to assess

their temporal variability and long-term trends with climate feedback mechanisms (Feng et al., 2017) and reduce the negative effects of excess irrigation water on crop production (Pôças et al., 2015). Evapotranspiration is the integration of two sections namely evaporation and transpiration that defined as the lost water from the soil surface and crop, respectively (Jensen and Allen, 2016). Several mathematical models used to determine the reference evapotranspiration ( $ET_0$ ). However, the method of Food and Agriculture Organization (FAO),

\* Corresponding author.

E-mail addresses: [ahmed\\_elbeltagi@zju.edu.cn](mailto:ahmed_elbeltagi@zju.edu.cn), [ahmedelbeltagy81@mans.edu.eg](mailto:ahmedelbeltagy81@mans.edu.eg) (A. Elbeltagi), [jsong\\_deng@zju.edu.cn](mailto:jsong_deng@zju.edu.cn) (J. Deng).

FAO-56 Penman – Monteith (Allen et al., 1998) is the most superior comparing to other (Gavila et al., 2007; Pereira et al., 2014; Tabari et al., 2013). But, it needs many climate data factors (Hobbins, 2016; Maroufpoor et al., 2020). Although  $ET_o$  can be estimated by this method most accurately, large scale meteorological data requirement at specific spatiotemporal scales (maximum and minimum air temperatures, wind speed, solar radiation, and vapor pressure deficit) are quite often not available in many developing countries (Almorox et al., 2015; Dadaser-celik et al., 2016; Espadafor et al., 2011; Irmak et al., 2012). Therefore, the alternate models are required for estimation of  $ET_o$  when the available data are either limited or insufficient. So, this study uses only temperature and solar radiation data as inputs to the alternative model.

The literature survey depicts that previously, several research studies have been focused on  $ET_o$  estimation using remote sensing (Farg et al., 2012), AquaCrop model (Butler et al., 2017; Li et al., 2016), FAO-CROPWAT (Surendran et al., 2015). However, the soft computing applications and analysis of big data techniques for actual evapotranspiration modeling are restrictive in the previous review literature. Numerous soft computing approaches have been widely applied to achieve the tractability, robustness, and provide a low-cost solution with a tolerance of imprecision, partial truth, uncertainty, and an approximation (Khoshravesh et al., 2017; Mehdizadeh et al., 2017; Motamedi et al., 2015). In agriculture field, analyzing big data have offered newly predictive models for  $ET_o$  estimation, for example, fuzzy-genetic and regularization random forest (Saggi and Jain, 2019a), firefly algorithm (Motamedi et al., 2015), adaptive neuro-fuzzy methodology (Gocic et al., 2015), convolution neural network (CNN) (Chen et al., 2020), hybrid models which use techniques such as data fusion and ensemble modeling, data decomposition as well as remote sensing-based hybridization (Chia et al., 2020), data-driven models (Kisi et al., 2015; Malik et al., 2019), wavelet conjunction heuristic (Kisi and Alizamir, 2018), artificial and wavelet neural networks (WNNs) based on temperature and wind speed data (Falamarzi et al., 2014), combination of Multivariate Adaptive Regression Splines (MARS) and Gene Expression Programming (GEP) models with autoregressive conditional heteroscedasticity (ARCH) time series model (Mehdizadeh, 2018), support vector regression coupled with nature-inspired algorithm (Mohammadi and Mehdizadeh, 2020; Tikhamarine et al., 2020, 2019), random forest and gene expression programming (Wang et al., 2019). The aforementioned methods produced satisfactory outcomes for estimation of evapotranspiration than the empirical models. Therefore, it is substantial to understand the temporal distributions of evapotranspiration and its projected changes using limited meteorological data and simple method. The proposed work contribute basic guidance to water-users and agricultural development planners for better assessing of  $ET_c$ , in the light of climate data availability, for the proper estimation of crop water demands.

To project the future changes in crop actual evapotranspiration, little researches have been conducted e.g., Xiao et al. (2018) used Agricultural Production Systems Simulator (APSIM) model and found that  $ET_c$  decreased across all stations under the two future climate scenarios (RCP4.5 and RCP8.5)., Mehdi and Vienna (2010) simulated the daily and the season total crop requirements using CROPWAT model and found a decrease of 2.71 % (8 mm), 21 % (64 mm) and 6% (59 mm) using the Statistical Downscaling Model (SDSM) with Canadian Centre for Climate Modelling and Analysis (CGCM1), and UK Hadley Centre for Climate Prediction and Research (HadCM3) using emission scenarios A2 and B2 predictors, respectively for the 2050s comparing with CROPWAT Model., Jeong et al. (2010) simulated  $ET_c$  based on artificial neural network (ANN) and HadCM3, and they found that the increasing  $ET_c$  gradually to 2099. Moreover, the agricultural water demand model was applied by Aladenola and Madramootoo (2010), and their findings showed that the percentage difference between future and current irrigation water needs ranged from -2 to 2%. Furthermore, SDSM was used by Li et al. (2012), and they found the

projected increase of 4% for the period 2011–2040. Chen et al. (2019) simulated the impacts of climate change on hydrology and crop production using an improved Soil and Water Assessment Tool (SWAT) model. Their results stated that annual  $ET_c$  and irrigation decreased by 8%–25 % and 15 %–42 %, respectively, under the climate change scenarios compared to the historical period. These models require many climatic data and geographical information for the prediction of  $ET_c$  process. In this study, deep neural network (DNN) was applied based on least climatic data, three climatic factors only for  $ET_c$  prediction in three governorates of Nile Delta region.

The most necessary issue to know about the deep learning approach is that the new features are learned and transformed through these deep neural architectures to increase the efficiency of the overall learning. DL can be used to model the complex relationship between input and output because of its high hierarchical structure model feature learning, construction, and training (Saggi and Jain, 2019b; Wang et al., 2018). The DNN method has been used in the agricultural and hydrological fields due to the difficulty of software data availability, costs and complexity, e.g., estimation and modeling of crop reference evapotranspiration(Ferreira and França, 2020; Saggi and Jain, 2019b), crop disease characterization (Lee et al., 2020; Ma et al., 2018), fast implementation of real-time detection (Kang and Chen, 2020; Zhang et al., 2019), automatic extraction of agricultural regulations (Espejo-Garcia et al., 2019), crop disease classification (Picon et al., 2018; Thenmozhi and Reddy, 2019), robotic precision farming (Kounalakis et al., 2019), automated training of trees on trellis wires (Majeed et al., 2020), hydroponics system (Mehra et al., 2018), flood prediction (Vinayaka and Suzanna, 2020), groundwater estimation from major physical hydrology components (Hassan et al., 2020), and runoff simulation (Fan et al., 2020).

Wheat as an important food security crop was selected in this study. It is the major winter cereal grain crop and the third major crop in terms of area planted in Egypt (FAO, 2011), accounting for 43 % of the total winter crop area (Sayed et al., 2019). In addition, there is a large gap between its production and consumption (Abdelmageed et al., 2019). Furthermore, to our knowledge, there are no studies available in the literature that evaluate the  $ET_c$  of wheat at the present and future in the semi-arid regions using deep learning. Hence, the aim of this research is (i) to analyze the temporal distributions of  $ET_c$  from 1970 to 2017, and (ii) to project the future changes in  $ET_c$  from 2022 to 2035 by employing the DNN method. This information is commanding to learn the impact of climate change on  $ET_c$  in the study region.

## 2. Materials and methods

### 2.1. Study area

The study area is located on the Nile Delta in Egypt. It occupies the northern part of Egypt where the Nile meets the Mediterranean Sea. The total length of the Nile River is approximately 7000 km, and it is known as the longest river in the world. The Nile Delta accounts for approximately 2 % of the total area of Egypt and contains up to 63 % of the agricultural land. The delta starts approximately 20 km north of Cairo and continues north for 150 km. The width of the delta is approximately 250 km and is bounded Alexandria governorate in the west and Port Said in the east. The annual mean maximum air temperature ( $T_{max}$ ) is 24 °C, and the annual mean minimum air temperature ( $T_{min}$ ) is 16 °C. The wind speed (WS) varies from 3.8 to 5.2 ms<sup>-1</sup>, and the rainfall season starts in October, representing approximately 75 % of the total rainfall. Most of the rainfalls occur in December and January, which are known as the雨iest months in this region (Shalaby, 2012; Shalaby and Tateishi, 2007). We selected three governorates in the Nile Delta, namely, Ad Daqahliyah, Ash Sharqiyah, and Kafr ash Shaykh with a total area of 11088 km<sup>2</sup>, as shown in Fig. 1. Wheat crop was selected for this study as one of the most important grain crops grown principally during the winter season in Egypt. The local production is

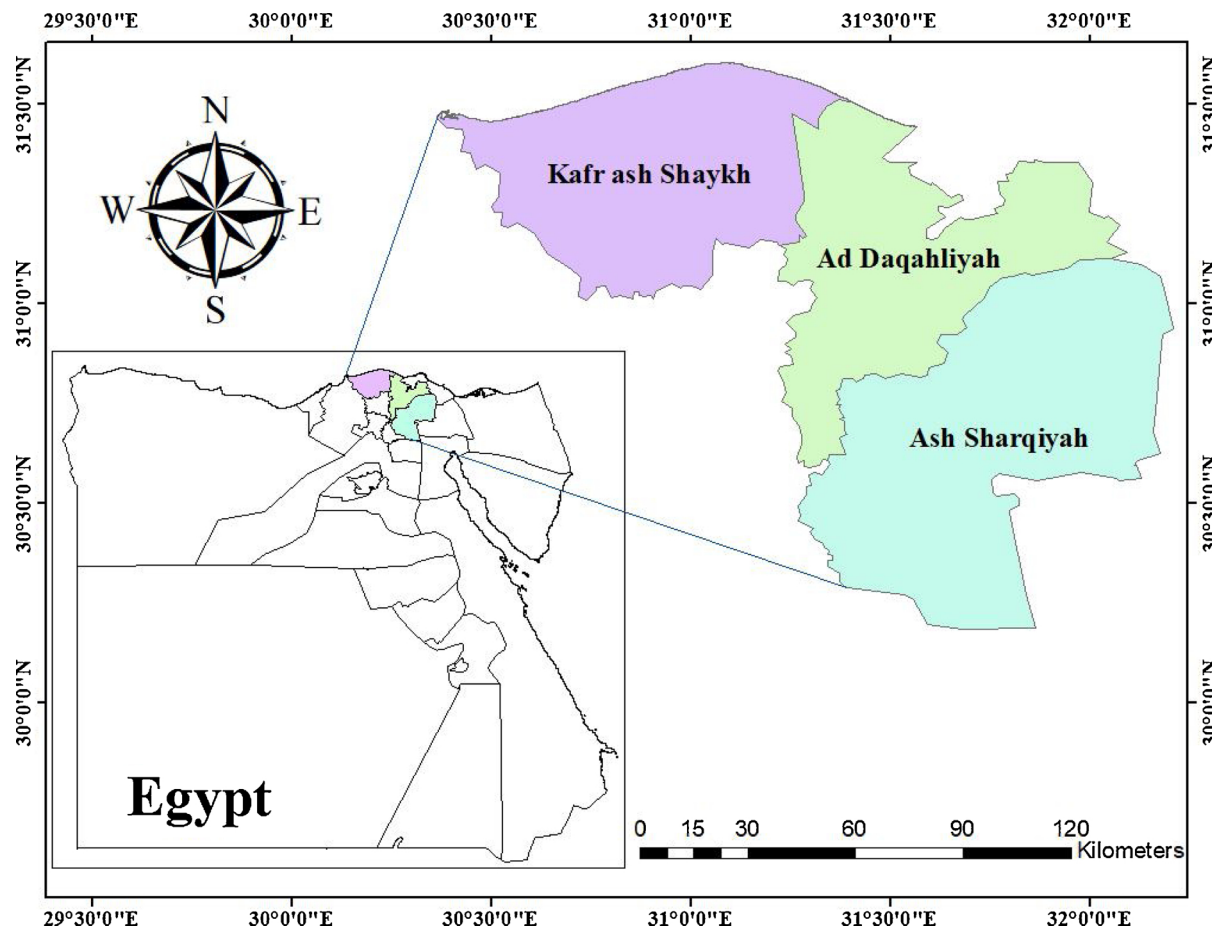


Fig. 1. Location map of study area.

not sufficient to supply the annual demand of the increasing population (Abdelmageed et al., 2019). Hence, increasing wheat production is the most important possibility for reducing the wheat gap and reach self-sufficiency of wheat production. We have collected the total agricultural crop-land areas of wheat for the three governorates from agriculture directorates of governorates and calculated the coverage of wheat crop in these regions. We found that wheat crop covers 35.72 %, 28.69 %, 39.71 % in the studied regions. According to the Food and Agricultural Organization (FAO) guidelines, the months for planting and harvesting wheat are from November to April. The length of crop growth stages are 40, 60, 60, and 40 days for initial, development, mid, and late periods, respectively (FAO, 2000).

## 2.2. Data sources

For historical data, the monthly data of maximum temperature ( $T_{\max}$ ), minimum temperature ( $T_{\min}$ ), precipitation (P), and solar radiation (SR) from November to April for wheat were extracted from open access data using Environmental Systems Research Institute (ESRI) Arc GIS tool over the period from 1970 to 2017 with a spatial resolution of about 4 km<sup>2</sup>. For more details about open access data, average maximum and minimum temperatures data were collected from Climatic Research Unit Ts 4.0 as Network Common Data Form (NetCDF) format at 0.5° grid for the global land surface (Abatzoglou et al., 2018). Furthermore, solar radiation data were collected from the Japanese 55-year Reanalysis JRA-55 as NetCDF format (Kobayashi et al., 2015).

For future climate data projection, General Circulation Models (GCMs) are physical-based tools that provide a reasonable basis for determining future climate data. However, the generated data from that

tool cannot be used directly in several regions or agricultural, water resources, and environmental researches due to poor simulation of local-scale processes (Masud et al., 2018). Thus, it is necessary to make downscaling of GCM output data before application in the impact studies, e.g., calibration of the DNN model. Three GCMs were obtained from the Coordinated Regional Climate Downscaling Experiment (CORDEX) initiative. This platform was developed by the World Climate Research Program (WCRP) to generate High-Resolution Climate Datasets (HRCD) over many locations worldwide (Gutowski et al., 2016). The  $T_{\max}$ ,  $T_{\min}$ , and SR data were obtained as monthly datasets from the Earth System Grid Federation (ESGF) over the period from 2022 to 2035. The ESGF portal allows user to discover data, and create scripts to fetch the data. Also, this system provides the full details about the selected variable and it's available as NetCDF format. The process for transferring a data set is for one variable for all realizations of one model for one experiment. Two Global Climate Models (GCMs): IPSL-CM5ALR (Institute Pierre-Simon Laplace) and MPI-ESM-MR (Max Planck Institute for Meteorology) were used as projections of climate change within the Coupled Model Inter comparison Project (Taylor et al., 2012). Besides, the Regional Climate Model (RCM) used was DMI HIRHAM5 and its driving GCM was ICHEC-EC-EARTH (Luhunga et al., 2018). Two extreme scenarios of the Representative Concentration Pathways, i.e., RCP 4.5, and RCP 8.5 were used as climate projections. CORDEX-RCM simulations for the African domain (AFR – CORDEX) are conducted at two different spatial resolutions, the general CORDEX resolution of 0.44 degree (AFR-44, ~50 km).

## 2.3. Calculation of crop evapotranspiration

To calculate reference evapotranspiration  $ET_o$ , the Hargreaves

method (HM) suggested by Food and Agricultural Organization (FAO) was used as illustrated in Eq. (1). This method was used because the parameters necessary to calculate the Penman-Monteith (PM) model are not available (Hargreaves and Allen, 2003; Aguilar et al., 2011; Fooladmand and Zandilak, 2008; Patel et al., 2014; Raziei and Pereira, 2013). The advantage of the HM over PM is that it only requires minimum and maximum temperatures, and solar radiation data, which may be easily obtained from available GIS-raster data.

$$ET_o = 0.0023 \times R_a (T_{\text{mean}} + 17.8)(T_{\text{max}} - T_{\text{min}})^{0.5} \quad (1)$$

Where:  $T_{\text{mean}}$  is the average temperature ( $^{\circ}\text{C}$ ),  $T_{\text{max}}$  is the maximum temperature ( $^{\circ}\text{C}$ ),  $T_{\text{min}}$  is the minimum temperature ( $^{\circ}\text{C}$ ) and  $R_a$  is extraterrestrial radiation (mm/month).

We then determined the crop coefficient using the thermal unit according to Eq. (2) by (Sammis et al., 1985). The equation established was equivalent to 0.12 for C value through the growing season, particularly for maize crop. But in this study, values of C were modified to match the wheat crop. C values were 0.05 for early-stage, 0.5 for the stem extension stage, 0.63 for the heading stage and -0.38 for the late stage. We also calibrated this equation over the period 1997–2007 to evaluate the performance level for calculating crop coefficients, and the validation was from 2008–2017.

$$K_c = C + 0.00168 \times T_u - 2.45 \times 10^{-7} \times T_u^2 - 4.37 \times 10^{-10} \times T_u^3 \quad (2)$$

Where: C is the constant depend on growth stage,  $T_u$  is a thermal unit as shown in Eq. (3), calculated based on air temperature and base temperature threshold of crop  $4.7^{\circ}\text{C}$  according to (Agrometeorological Centre of Excellence, 2020; Barger, 1969).

$$T_u = \sum_{i=1}^n \frac{T_{\text{max}} + T_{\text{min}}}{2} - T_{\text{base}} \quad (3)$$

By the available data obtained from crop coefficients, the crop evapotranspiration is calculated according to the simple equation ( $ET_c = ET_o \times K_c$ ).

#### 2.4. Temporal analysis of crop evapotranspiration

Open GeoDa is a software package prepared to produce spatial data analysis, is an open-source successor to GeoDa. GeoDa was designed under the auspices of the National Science Foundation (NSF) funded Center for Spatially Integrated Social Science (Anselin et al., 2006). It was used to interpret the spatial distribution of  $ET_c$  for the long term. The collected data of minimum and maximum temperatures and solar radiation during 1970–2017 are interpolated to show the present spatial-temporal changes for the three studied locations.

#### 2.5. Projection of crop evapotranspiration

Historical data were divided into two segments as input variables for the artificial intelligence model, from 1970 to 2000 for the training and 2001–2017 for the validating. The Deep neural network (DNN) was applied using Visual Gene Developer (VGD) software version 1.9 (Jung and McDonald, 2011), as shown in the interface (Fig. 2). The DNN is designed from many types of layers: (1) the input layer is the initial data for DNN, (2) the hidden layers are intermediate layers between the independent input and dependent output layers where all the computations are done, and (3) the output layer produces the result for the given inputs (Elbeltagi et al., 2020a). The software not only provides general functions for gene analysis and optimization along with an interactive user-friendly interface, but also includes unique features such as programming capability, dedicated mRNA secondary structure prediction, artificial neural network modeling, network & multi-threaded computing, and user-accessible programming modules. The software allows a user to analyze and optimize a sequence using main menu functions or specialized module windows. Alternatively, gene

optimization can be initiated by designing a gene construct and configuring an optimization strategy. A user can choose several predefined or user-defined algorithms to design a complicated strategy. The software provides expandable functionality as platform software supporting module development using popular script languages such as VBScript and JScript in the software programming environment. It is an available free download at <http://visualgenedeveloper.net/>. This method was calibrated at three hidden layers (10 nodes/layer), learning rate (0.003), momentum coefficient (0.1), transfer function (Hyperbolic tangent), target error (0.00001), initialization method of threshold and weight factor (Random), and analysis update interval (500 iterations). There are five type of transfer functions including Sigmoid, Tangent, Hyperbolic tangent, Gaussian, and Linear. In the present study, the Hyperbolic tangent function and other model parameters were selected based on the lowest RMSE, which is a common procedure in literature (Maroufpoor et al., 2019a, 2019b). Finally future data from 2022 to 2035 were added in the prediction set to simulate future crop evapotranspiration under the impacts of the two-climate change scenarios. A layout of the adopted methodology is shown in Fig. 3.

#### 2.6. Performance evaluation

The actual and predicted  $ET_c$  values were compared throughout the study period. To evaluate the performance of the DNN model, the following statistical indicators were selected: mean square error (MSE), root mean square error (RMSE), mean absolute error (MAE), mean absolute relative error (MARE), mean absolute percentage error (MAPE), Accuracy (Acc), Nash-Sutcliffe efficiency (NSE) (Elbeltagi et al., 2020a; Saggi and Jain, 2019b; Yamaç and Todorovic, 2020; Tao et al., 2015; Seyedzadeh et al., 2019). All these indicators are defined as follows:

##### 1 Mean square error (MSE)

$$\text{MSE} = \frac{1}{N} \sum_{i=1}^N (ET_{c,Act}^i - ET_{c,P}^i)^2 \quad (4)$$

##### 2 Root mean square error (RMSE)

$$\text{RMSE} = \sqrt{\frac{1}{N} \sum_{i=1}^N (ET_{c,Act}^i - ET_{c,P}^i)^2} \quad (5)$$

##### 3 Mean absolute error (MAE)

$$\text{MAE} = \frac{1}{N} \sum_{i=1}^N |(ET_{c,Act}^i - ET_{c,P}^i)| \quad (6)$$

##### 4 Mean absolute percentage error (MAPE)

$$\text{MAPE} = 100 \times \frac{1}{N} \sum_{i=1}^N \frac{|(ET_{c,Act}^i - ET_{c,P}^i)|}{ET_{c,Act}^i} \quad (7)$$

##### 5 Mean absolute relative error (MARE)

$$\text{MARE} = \sum_{i=1}^N \frac{|(ET_{c,Act}^i - ET_{c,P}^i)|}{ET_{c,Act}^i} \quad (8)$$

##### 6 Accuracy (Acc)

$$\text{Acc} = 1 - \text{abs}(\text{mean} \frac{ET_{c,P}^i - ET_{c,Act}^i}{ET_{c,Act}^i}) \quad (9)$$

##### 7 Nash-Sutcliffe efficiency (NSE)

$$\text{NSE} = 1 - \sum_{i=1}^N \frac{(ET_{c,Act}^i - ET_{c,P}^i)^2}{(ET_{c,Act}^i - ET_{c,-}^i)^2} \quad (10)$$

Where  $ET_{c,A}$  is the actual or observed value,  $ET_{c,P}$  is the predicted value,  $ET_{c,-}$  is the mean value, and N is the total number of data points.

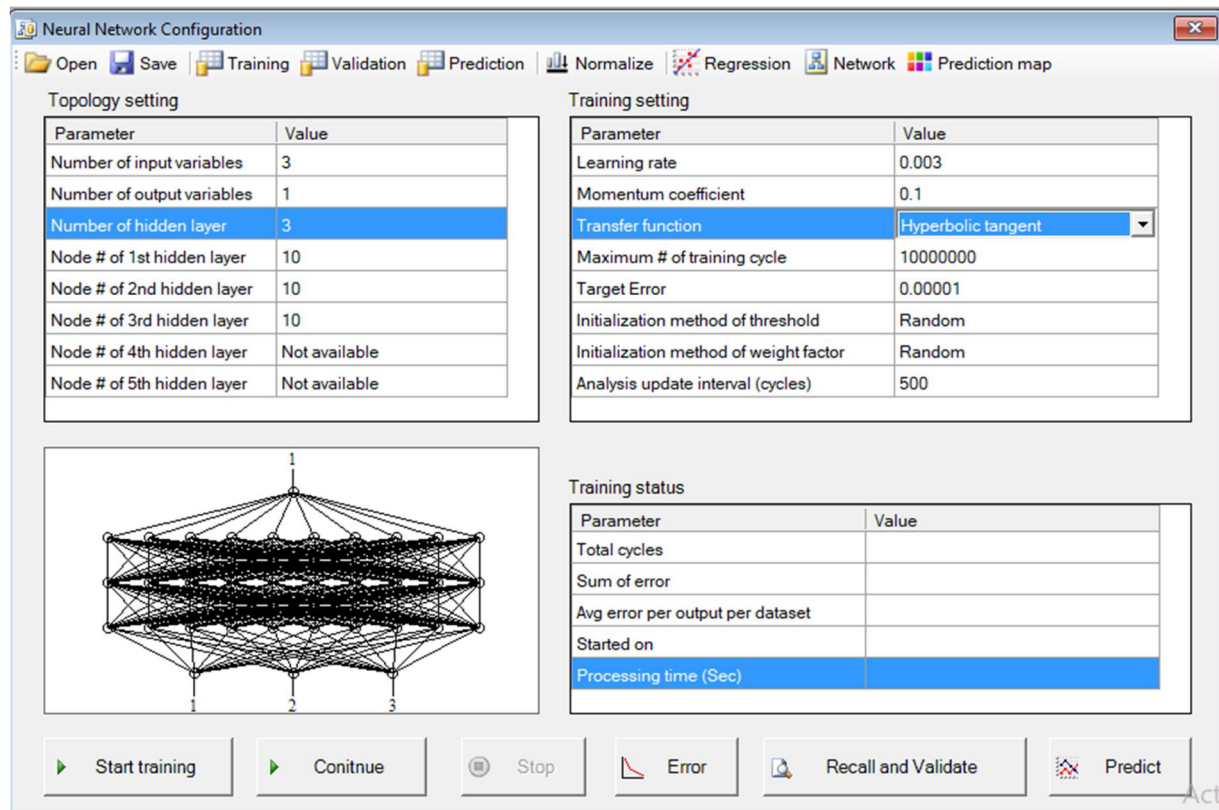


Fig. 2. The interface of deep neural networks.

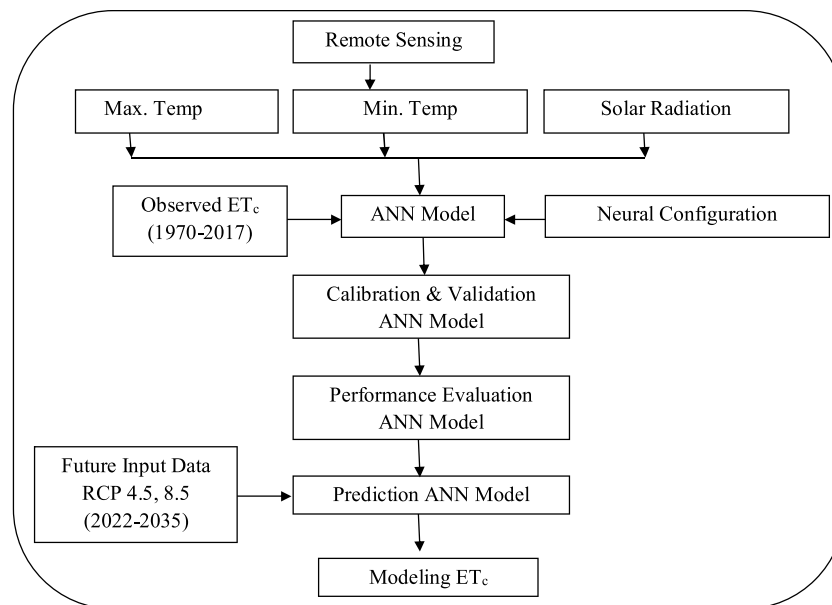


Fig. 3. A schematic diagram of the adopted methodology.

### 3. Results

#### 3.1. Temporal changes of climatic parameters during 1970–2017

The average annual of minimum and maximum temperatures and solar radiation data during the calibration and validation datasets are shown in Fig. 4. For maximum temperature ( $T_{\max}$ ) analysis during the calibrated years from 1970–2000, the highest temperature values are found in the Ad Daqahliyah region, which is more than 33 °C. While the

lowest temperature values in Kafr ash Shaykh is less than 27 °C. The mean maximum temperatures were 25.43 °C, 22.23 °C, and 21.64 °C in Ad Daqahliyah, Kafr ash Shaykh, and Ash Sharqiyah, respectively. Meanwhile,  $T_{\max}$  values through the validated years from 2000–2017 were 26.74 °C, 27.36 °C, and 27.52 °C with an average of 22.79 °C, 23.16 °C, and 22.59 °C for Ad Daqahliyah, Kafr ash Shaykh, and Ash Sharqiyah, respectively. In addition, the temporal changes of seasonal minimum temperature ( $T_{\min}$ ) show a mixed pattern of upward and downward trend on the studied regions during the calibrated and

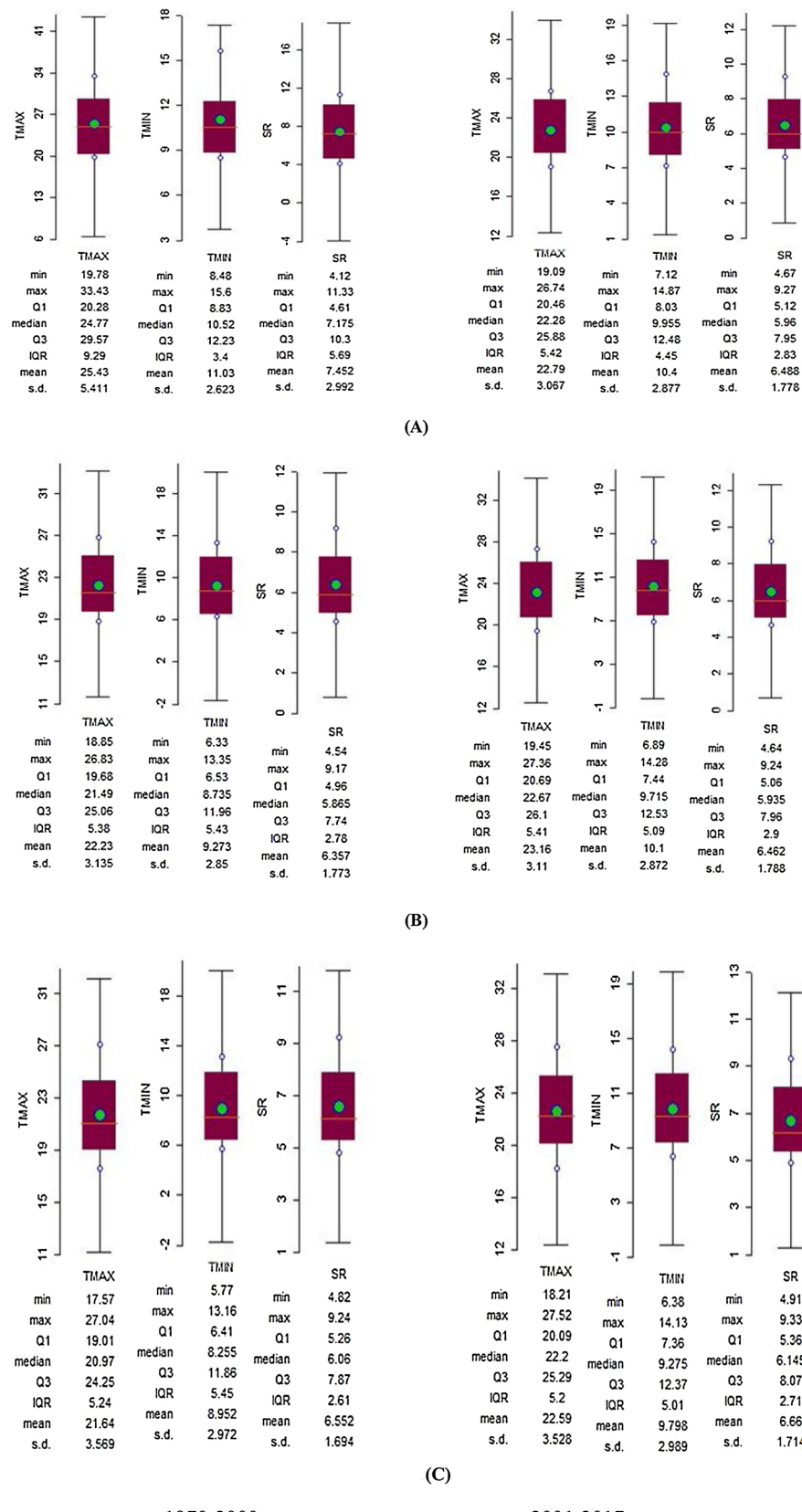


**Fig. 4.** Spatial and temporal changes through the calibration (1970-2000) and validation (2001-2017) periods for (A) Ad Daqahliyah, (B) Kafr ash Shakhyh, and (C) Ash Sharqiyah.

**Table 1**

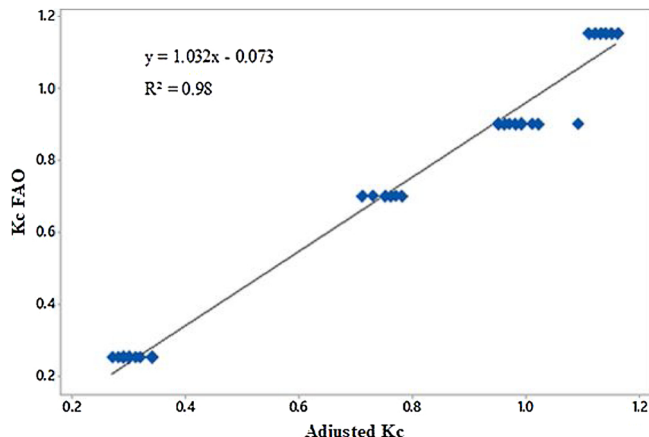
Descriptive statistics of the collected data from 1970–2017 for the three studied governorates.

Variable	Mean	SE Mean	St Dev	Minimum	Q1	Median	Q3	Maximum
<b>A. Ad Daqahliyah</b>								
Tmax	22.13	0.182	3.08	16.2	19.5	21.55	25.07	28.8
Tmin	9.82	0.167	2.84	4	7.6	9.35	12	17
SR	6.41	0.096	1.63	3.98	5.04	5.85	7.82	9.58
Tmean	15.97	0.171	2.91	10.25	13.65	15.37	18.77	22.1
<b>B: Ash Sharqiyah</b>								
Tmax	21.95	0.206	3.49	15.4	19.03	21.4	24.87	29.6
Tmin	9.23	0.173	2.94	3.3	6.9	8.6	11.9	16.2
SR	6.58	0.092	1.57	4.34	5.29	5.99	7.93	9.58
Tmean	15.59	0.186	3.15	9.45	12.96	14.9	18.7	22.05
<b>C. Kafr ash Shaykh</b>								
Tmax	22.54	0.183	3.11	16.7	20	21.8	25.4	29.5
Tmin	9.54	0.166	2.82	3.9	7.23	9.1	12	16.4
SR	6.39	0.097	1.64	3.98	5	5.85	7.82	9.55
Tmean	16.04	0.172	2.92	10.5	13.71	15.45	18.9	22.1

SE Mean: Standard Error of mean, St Dev: Standard deviation, Q1: First Quartile, Median: Middle number, Q3: Third Quartile.

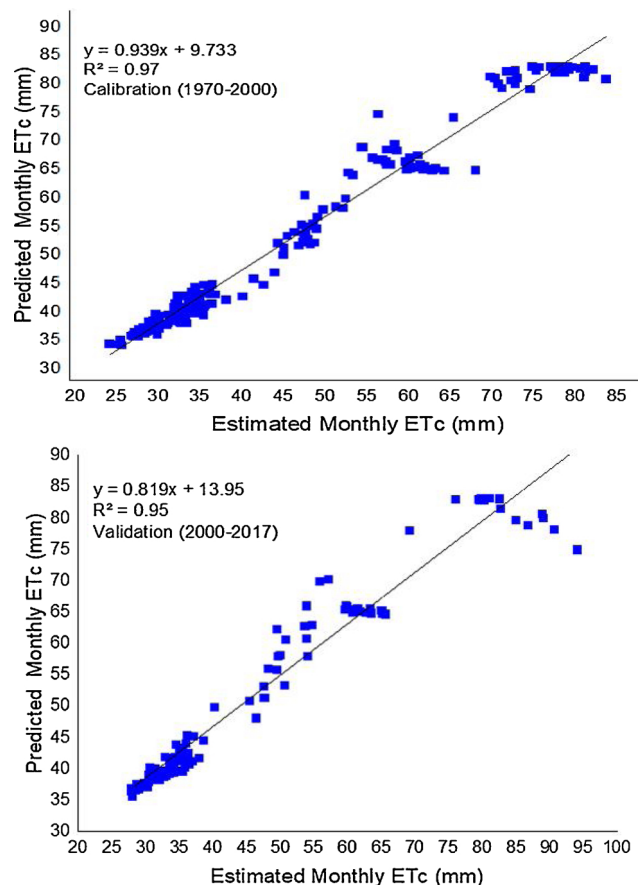
**Table 2**Average crop coefficient ( $K_c$ ) values of wheat at different growing stages for calibration, validation, and prediction periods in the three study regions.

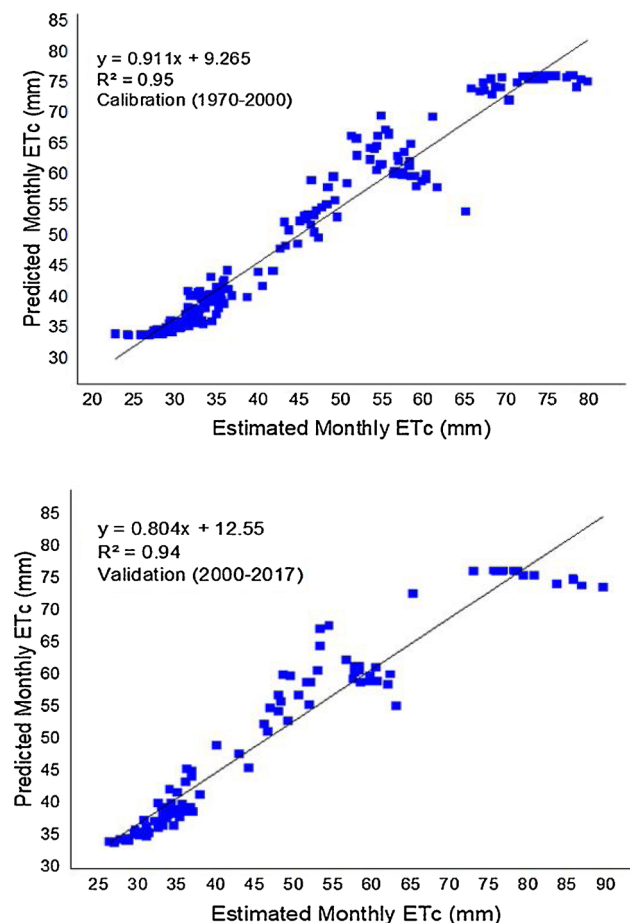
Period	Ad Daqahliyah				Kafr ash Shaykh				Ash Sharqiyah			
	Initial	Dev	Mid	Late	Initial	Dev	Mid	Late	Initial	Dev	Mid	Late
1970–2000	0.72	1.01	1.15	0.34	0.71	0.98	1.14	0.31	0.76	0.95	1.13	0.29
2000–2017	0.78	0.97	1.13	0.3	0.73	0.96	1.15	0.34	0.78	0.99	1.14	0.32
2022–2035	0.74	1.02	1.16	0.28	0.75	1.09	1.12	0.27	0.77	0.99	1.11	0.31

Fig. 5. Comparison between average calculated and recommended  $K_c$  values.

validated years. An upward trend was recorded 15.6 and 14.87 °C as maximum of  $T_{\text{min}}$  in Ad Daqahliyah regions compared with other regions, which were 13.35 °C, and 14.28 °C for Kafr ash Shaykh and 13.16 °C, 14.16 °C for Ash Sharqiyah. Moreover, the downward trends were values of 8.48 °C and 7.12 °C in Ad Daqahliyah, 6.33 °C and 6.89 °C in Kafr ash Shaykh, and 5.77 °C and 6.38 °C in Ash Sharqiyah. The temporal changes of minimum and maximum temperatures affected directly on solar radiation (SR) values during the studied years, which was reached to a high value of 11.33 mm/day with a mean value of 7.45 mm.day<sup>-1</sup> in Ad Daqahliyah from 1970–2000 compared with other regions. As well, the Ash Sharqiyah region was the highest SR value, which was 9.33 °C with a mean value of 6.66 °C during 2000–2017. The descriptive statistics of the collected data from 1970 to 2017 for the three study governorates are listed in Table 1.

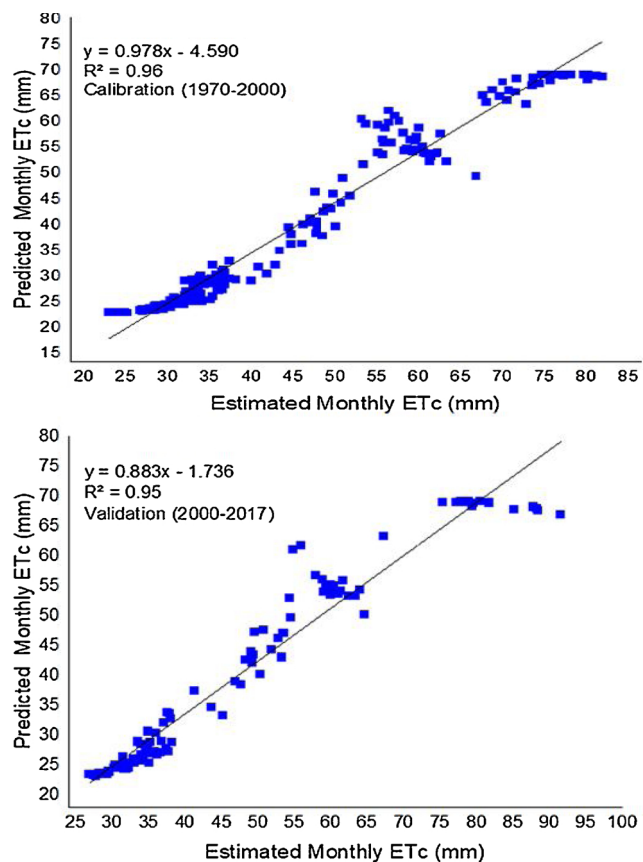
After understanding the temporal distribution of climatic factors, much important information can be provided for analyzing the trend of crop actual evapotranspiration ( $ET_c$ ) based on the Hargreaves method.

Fig. 6. Actual versus predicted monthly  $ET_c$  in Ash Sharqiyah during calibration and validation periods.



**Fig. 7.** Actual versus predicted monthly  $ET_c$  in Ad Daqahliyah during calibration and validation periods.

As shown in Table 2,  $K_c$  values of wheat were presented at different growing stages i.e., initial, development, mid, and late for calibration, validation, and prediction periods in the three study regions. Then, the  $K_c$  values obtained from the followed method were evaluated with recommended FAO- $K_c$ . The coefficient of determination between calculated and recommended was found to be 0.98 as shown in Fig. 5. The findings showed that the monthly  $ET_c$  values were recorded highest values in Ash Sharqiyah more than 80 mm (Fig. 6) then Ad Daqahliyah, which was more than 75 mm (Fig. 7) comparing to the third location (Fig. 8). Furthermore, we compared the predicted monthly  $ET_c$  with the values calculated by the Hargreaves method for the validation period from 2000–2017 for the three governorates (Tables 3–5). The results showed that in Ad Daqahliyah region the highest accuracy and NSE of 0.94 and 0.96 were recorded in 2015 with low statistical error ( $RMSE = 3.21 \text{ mm.month}^{-1}$ ,  $MAE = 2.98 \text{ mm.month}^{-1}$ ,  $MAPE = 7.86\%$ , and  $MARE = 0.06 \text{ mm.month}^{-1}$ ) compared to the years of 2002 and 2003 (Table 3). In addition, the high performance of DNN model in Kafr ash Shaykh was found in 2000 with 0.90 for accuracy and NSE in comparison with the results of 2008 and 2010 that achieved the lowest performance (Table 4). For the third governorate (Ash Sharqiyah), the year of 2015 was the best for predicting the  $ET_c$  ( $RMSE = 4.71 \text{ mm.month}^{-1}$ ,  $MAE = 4.11 \text{ mm.month}^{-1}$ ,  $MARE = 0.08 \text{ mm/month}$ ,  $MAPE = 11.05\%$ ,  $Acc = 0.92$ , and  $NSE = 0.93$ ) as listed in Table 5. Also, the lowest accuracy and NSE were estimated in 2002 ( $NSE = 0.76$ ). As averages of the calibration and validation years, the relationship between the predicted versus actual wheat  $ET_c$  produced satisfactory results. The coefficient of determination, slope, and intercept are 0.95, 0.91, and 9.27 for Ad Daqahliyah, 0.96, 0.98, and -4.59 for Kafr ash Shaykh, and 0.97, 0.94, and 9.73 for Ash Sharqiyah,



**Fig. 8.** Actual versus predicted monthly  $ET_c$  in Kafr ash Shaykh during calibration and validation periods.

**Table 3**

Comparison between the predicted and actual crop evapotranspiration over 2000–2017 in Ad Daqahliyah.

Years	Actual (mm)	Predicted (mm)	MSE (mm)	RMSE (mm)	MAE (mm)	MAPE (%)	MARE (mm)	Acc	NSE
2000	290.13	317.04	38.17	6.17	5.14	13.27	0.1	0.9	0.87
2001	294.67	310.81	57.78	7.6	6.64	14.77	0.13	0.87	0.84
2002	275.6	316.07	71.18	8.43	7.58	18.52	0.16	0.84	0.78
2003	265.96	300.15	35.89	5.99	5.69	13.97	0.12	0.88	0.78
2004	287.96	302.09	40.23	6.34	5.55	12.83	0.11	0.89	0.88
2005	283.96	305.66	28.28	5.14	5	11.98	0.1	0.9	0.9
2006	285.41	304.79	28.89	5.37	5.04	12.27	0.1	0.9	0.9
2007	277.56	300.53	21.52	4.64	4.02	11.33	0.08	0.92	0.92
2008	296.68	299.42	88.89	9.43	8.51	17.18	0.17	0.83	0.8
2009	292.41	312.68	18.65	4.31	3.41	8.73	0.07	0.93	0.92
2010	301.78	304	31.38	5.6	4.57	9.32	0.09	0.91	0.91
2011	285.59	317.01	46.01	6.78	5.23	11.82	0.11	0.89	0.79
2012	274.01	294.94	23.35	4.83	4.67	12.11	0.1	0.9	0.91
2013	295.84	303.68	46.7	6.83	5.69	11.35	0.11	0.89	0.88
2014	288.05	308.29	20.06	4.47	3.63	9.85	0.07	0.93	0.93
2015	277.03	290.32	10.31	3.21	2.98	7.86	0.06	0.94	0.96
2016	285.29	302.43	21.93	4.68	4.33	11.45	0.09	0.91	0.93
2017	275.77	303.21	29.13	5.39	4.67	13.28	0.1	0.9	0.9

MSE: Mean square error, RMSE: Root mean square error, MAE: Mean absolute error, MARE: Mean absolute relative error, MAPE: Mean absolute percentage error, Acc: Accuracy, NSE: Nash-Sutcliffe efficiency.

respectively for the calibration period. Additionally, for the validation period, the corresponding values were 0.94, 0.80, and 12.55 in Ad Daqahliyah, 0.95, 0.88, -1.74 in Kafr ash Shaykh, and 0.95, 0.82, and 13.95 in Ash Sharqiyah, respectively.

**Table 4**

Comparison between the predicted and actual crop evapotranspiration over 2000–2017 in Kafr ash Shaykh.

Years	Actual (mm)	Predicted (mm)	MSE (mm)	RMSE (mm)	MAE (mm)	MAPE (%)	MARE (mm)	Acc	NSE
2000	267.1	247.6	25.17	5.01	4.6	10.64	0.1	0.9	0.9
2001	302.82	253.81	99.87	9.99	8.16	15.81	0.16	0.84	0.74
2002	282.14	259.74	42.38	6.51	5.8	13.21	0.12	0.88	0.87
2003	272.14	239.47	38.62	6.21	5.44	13.71	0.12	0.88	0.78
2004	294.43	246.12	83.25	9.12	8.05	16.53	0.16	0.84	0.77
2005	290.36	248.35	59.27	7.67	7	15.63	0.14	0.86	0.81
2006	291.45	247.9	60.18	7.75	7.25	15.73	0.15	0.85	0.81
2007	284.37	242.54	52.77	7.26	6.97	15.66	0.14	0.86	0.82
2008	303.08	242.49	157.92	12.56	10.09	18.85	0.2	0.8	0.67
2009	299.16	253.59	59.43	7.7	7.59	16.53	0.15	0.85	0.76
2010	309.72	246.84	129.17	11.36	10.47	20.59	0.2	0.8	0.65
2011	292.03	258.37	61.59	7.84	7.53	16.89	0.15	0.85	0.73
2012	280.52	237.35	54.08	7.35	7.19	16.79	0.15	0.85	0.82
2013	303.16	248.29	114.02	10.67	9.14	18.7	0.18	0.82	0.72
2014	294.5	250.68	56.73	7.53	7.3	16.23	0.14	0.86	0.81
2015	282.96	232.95	75.46	8.68	8.33	19.34	0.17	0.83	0.75
2016	291.87	246.14	62.36	7.89	7.61	16.62	0.16	0.84	0.82
2017	282.75	245.96	40.69	6.37	6.13	13.97	0.13	0.87	0.87

MSE: Mean square error, RMSE: Root mean square error, MAE: Mean absolute error, MARE: Mean absolute relative error, MAPE: Mean absolute percentage error, Acc: Accuracy, NSE: Nash–Sutcliffe efficiency.

**Table 5**

Comparison between the predicted and actual crop evapotranspiration over 2000–2017 in Ash Sharqiyah.

Years	Actual (mm)	Predicted (mm)	MSE (mm)	RMSE (mm)	MAE (mm)	MAPE (%)	MARE (mm)	Acc	NSE
2000	293.82	323.31	37.62	6.13	5.87	14.63	0.12	0.88	0.89
2001	302.44	328.72	60.08	7.75	7.39	17	0.14	0.86	0.85
2002	285.43	334.93	85.99	9.27	8.25	20.44	0.17	0.83	0.76
2003	276.58	316.63	47.25	6.87	6.67	15.76	0.14	0.86	0.77
2004	296.72	322.36	50.33	7.09	6.93	16.22	0.14	0.86	0.87
2005	293.08	326.39	41.63	6.45	6.01	15.09	0.12	0.88	0.87
2006	295.8	323.86	44.39	6.66	6.46	15.79	0.13	0.87	0.88
2007	285.37	322.9	45.14	6.71	6.25	16.42	0.13	0.87	0.85
2008	307.01	321.99	116.77	10.8	9.25	19.55	0.18	0.82	0.77
2009	304.76	339.72	40.16	6.33	5.82	13.66	0.11	0.89	0.85
2010	312.95	327.46	32.85	5.73	5.16	11.47	0.09	0.91	0.92
2011	295.88	335.39	57.08	7.55	6.58	14.76	0.13	0.87	0.77
2012	284.76	318.82	41.08	6.41	5.87	15.23	0.12	0.88	0.86
2013	307.7	323.33	55.67	7.46	6.84	14.09	0.13	0.87	0.87
2014	297.77	331.09	37.31	6.1	5.55	13.82	0.11	0.89	0.88
2015	288.64	313.35	22.17	4.71	4.11	11.05	0.08	0.92	0.93
2016	294.34	324.93	35.11	5.92	5.09	14.2	0.1	0.9	0.91
2017	285.63	323.3	44.08	6.63	6.27	16.61	0.13	0.87	0.87

MSE: Mean square error, RMSE: Root mean square error, MAE: Mean absolute error, MARE: Mean absolute relative error, MAPE: Mean absolute percentage error, Acc: Accuracy, NSE: Nash–Sutcliffe efficiency.

### 3.2. Projected changes in wheat evapotranspiration during 2022–2035

The projected increase in climatic factors under the average two scenarios is greater than the average of historical period from 1970 to 2017. The increase in temperature was attributed to the increase of  $T_{\max}$  degrees from 22.29 °C to 25.43 °C, 22.11 °C–23.09 °C, and 22.69 °C–28.66 °C, respectively for Ad Daqahliyah, Ash Sharqiyah, and Kafr ash Shaykh. The corresponding  $T_{\min}$  degrees also increased from 9.97 °C to 11.03 °C, from 9.37 °C to 14.75 °C and from 9.68 °C to 13.41 °C, respectively. For the three regions, SR values also increased from 6.43 to 7.45 mm day<sup>-1</sup>, from 6.61 to 8.13 mm day<sup>-1</sup> and from 6.41 to 9.01 mm day<sup>-1</sup>, respectively.  $T_{\max}$  will increase by 5.19 %, 4.22 %, and 20.82 % for Ad Daqahliyah, Ash Sharqiyah, and Kafr ash Shaykh, respectively (Fig. 9). Whereas, their corresponding average values of  $T_{\min}$  will increase by 1.62 %, 36.44 %, and 27.80 %, respectively. The highly increase in  $T_{\min}$  and  $T_{\max}$  data affected directly on the expected solar radiation (SR) values as stated by Elbeltagi et al. (2020b). It would increase by 6.53 %, 18.74 %, and 28.83 % for the corresponding regions as mentioned above, respectively (Fig. 9).

After the calibration and validation of the DNN model based on the climate data scenarios (RCP 4.5 and 8.5) during the historical periods that incorporated to the DNN method, the predicted wheat  $ET_c$  from 2022–2035 based on future data for the three studied regions as illustrated in Table 6. The projected  $ET_c$  values vary due to climate variations between  $T_{\max}$ ,  $T_{\min}$ , and SR in RCP 4.5 and RCP 8.5 with averages of 1.22 °C, 1.78 °C, and 0.91 mm day<sup>-1</sup>. The results showed that Kafr ash Shaykh governorate produced the highest values of  $ET_c$  during the future period, which is averaged from 302.03 in 2024 to 329.68 in 2032. The average value of  $ET_c$  during 1970–2017 and 2022–2035 was 281.84 mm and 313.72 mm with an increase by 11.31 % (Fig. 10). Then, the Ad Daqahliyah was the second rank, which is ranged from 262.98 in 2031 to 301.53 in 2026. The corresponding percent increased of  $ET_c$  is 1.38 % compared to the historical data. As well, the lowest values of  $ET_c$  were in Ash Sharqiyah region that varied from 204.05 in 2025 to 281.47 in 2035. Average across the two scenarios for the Ash Sharqiyah area,  $ET_c$  would decrease by 15.09 % from 285.02 mm to 242.02 mm (Fig. 10). The results stated that the DNN model performs well in reproducing the present  $ET_c$  and can be used as

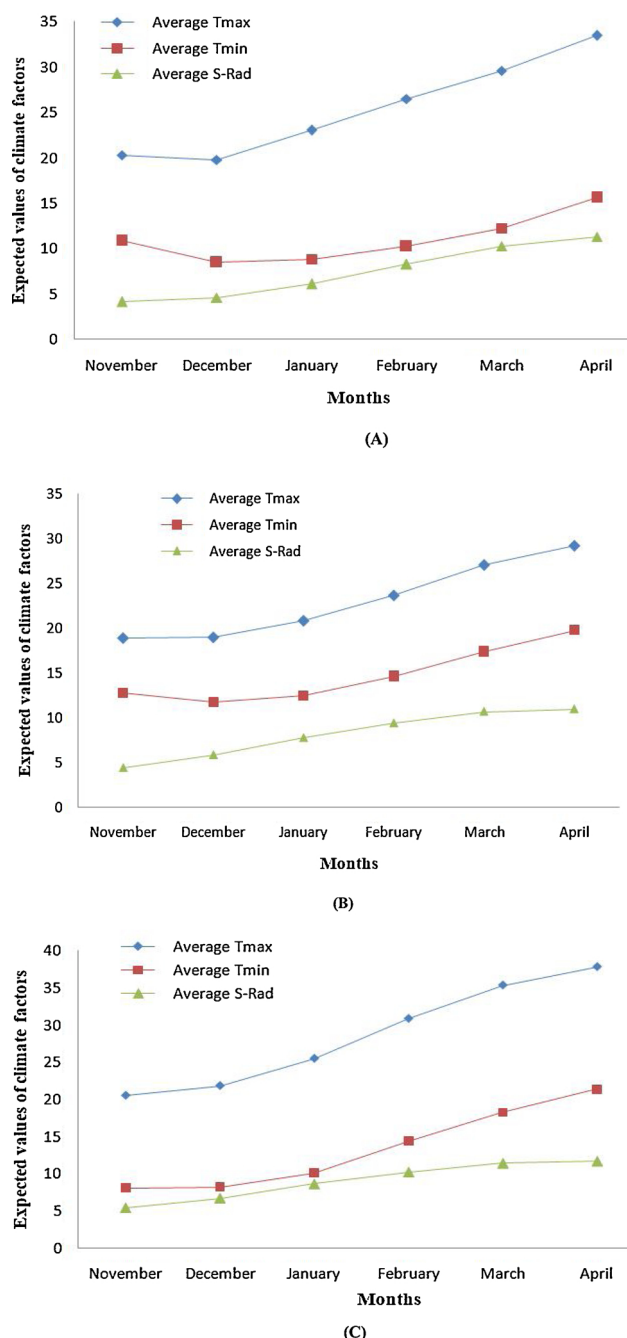


**Fig. 9.** Average of expected maximum and minimum temperatures ( $T_{\text{max}}$  and  $T_{\text{min}}$ ) and solar radiation (SR) values based on the climatic scenarios over the period from 2022-2035 for (A) Ad Daqahliyah, (B) Ash Sharqiyah, and (C) Kafra ash Shaykh.

a robust and reliable tool to project future  $\text{ET}_c$  using limited climate data.

#### 4. Discussion

Crop evapotranspiration values of wheat predicted based on the followed method in this study were compared to actual during calibration and validation periods as discussed earlier in section 3.1. FAO suggested the  $K_c$  values for the initial, development, mid, and late stages of the crop are 0.7, 0.9, 1.15, and 0.25 (FAO, 2000). The  $K_c$  values are appropriate with FAO through the growing season are 0.72, 0.88, 1.13 and 0.32. These findings are similar to those of Farg et al.

(2012), who indicated that the determination coefficients ( $R^2$ ) between combination of Soil-Adjusted Vegetation Index (SAVI) and Normalized Difference Vegetation Index (NDVI) as spectral vegetation indices for estimating  $K_c$  were 0.827, 0.903, and 0.976 through initial, mid, and last growth stages, respectively. In addition, these findings were better than Pócas et al. (2015) who found that the  $R^2$  between reflectance-based vegetation indices and soil water balance SIMDual model was 0.72. Our results have achieved high performance compared to Anwer et al. (2016), reported that the average relative error values between the approximate values of  $K_c$  and FAO were 36.29 %. In addition, the results obtained are in line with Elbeltagi et al. (2020b), who modeled  $K_c$  values using  $T_{\text{min}}$ ,  $T_{\text{max}}$ , and SR and produced satisfactory output with high accuracy and less statistical error. Moreover, our  $K_c$  results are good in comparison with Mulovhedzi et al. (2020), who estimated  $K_c$  values based on Growing Degree Days (GDD) only and found the equation was successfully validated by comparing measured against estimated  $K_c$  with an  $R^2 = 0.80$  and mean absolute percent difference (MAPD) = 7%. In addition, these results imply that the reference  $\text{ET}_c$  is more sensitive to  $T_{\text{min}}$ ,  $T_{\text{max}}$  and SR, which consistent with the similar studies conducted in West Texas (Awal et al., 2020), Kaduna Central District (Onwuegbunam et al., 2020), Pearl River Basin (Huang et al., 2020), and in the semi-arid region of South India (Gonzalez et al., 2020).

In addition, the current followed method for prediction of wheat  $\text{ET}_c$  are close to Chen et al. (2020), who applied the temporal convolution-network model for predicting  $\text{ET}_c$  and generated well output with  $R^2$  ranged from 0.91 to 0.95. Moreover, the research findings are similar to the outputs of fuzzy-genetic and regularization random forest models presented by Saggi and Jain (2019a), they found that the models had high performance for modeling  $K_c$  and  $\text{ET}_c$  (e.g. RMSE = 0.1160–0.396,  $R^2 = 0.830–0.99$ ,  $A_{\text{cc}} = 94\%–99\%$ ). As well, our findings are in agreement with Yamaç and Todorovic (2020), they employed the different machine learning (ML) models based on limited climate data, and results reveals the satisfactory outputs of ML with  $R^2$  ranged from 0.81 to 0.97. Moreover, the results are in line with Everton et al. (2020), evaluated the performance of the Simple Algorithm for Evapotranspiration Retrieving (SAFER) using missing meteorological data. Their findings stated that  $R^2$  ranged from 0.95 to 0.97 at missing any data of solar radiation, wind speed, and relative humidity. Additionally, the developed model produced satisfactory outputs compared to Maselli et al. (2020), used an improved normalized difference vegetation index (NDVI) based on Fractional Vegetation Cover and stated that  $R^2$  increased from 0.814 to 0.933, while RMSE decreased from 1.73 to 0.57 mm. Also, this study gave similar results with Falamarzi et al. (2014) outputs, they estimated ET based on temperature and wind speed data using artificial and wavelet neural networks (WNNS) and found the best model produced high NSE (0.79),  $R^2$  (0.89), and low RMSE (1.03 mm/day). Furthermore, the DNN outputs agree well with that of Kisi and Alizamir (2018), applied the wavelet extreme learning machine (WELM) model for modeling evapotranspiration and found high  $R^2$  as 0.97 and 0.96 for model during training and testing with the combination of solar radiation, mean air temperature, relative humidity, and wind speed. In addition, the results are in line with Kisi (2016), who observed that the M5 model tree produced the best alternative with high correlation with Penman Monteith method for estimating evapotranspiration in the absence of local input and output data. Besides, the generated DNN results are in agreement with the findings of Khoshravesh et al. (2017), estimated monthly ET using the multivariate fractional polynomial, robust regression, and Bayesian regression models and concluded that all models provided a closer agreement with the calculated values for FAO-PM ( $R^2 = 0.95$  and RMSE = 12.07 mm month $^{-1}$ ).

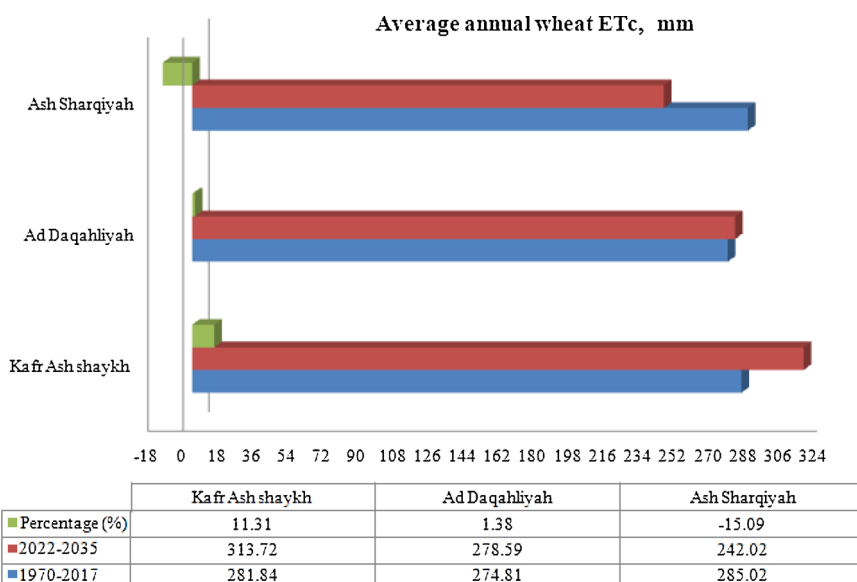
#### 5. Conclusions

This research evaluates the effects of historical and future climate

**Table 6**

The predicted data based on the two scenarios of climate data and their averages for the three governorates from 2022–2035.

Year	Ad Daqahliyah			Kafr Ash Shaykh			Ash Sharqiyah		
	ETc, mm RCP 8.5	ETc, mm RCP 4.5	Average, mm	ETc, mm RCP 8.5	ETc, mm RCP 4.5	Average, mm	ETc, mm RCP 8.5	ETc, mm RCP 4.5	Average, mm
2022	277.05	267.7	272.37	300.89	308.39	304.64	244.54	226.6	235.57
2023	273.23	283.21	278.22	295.34	315.25	305.29	223.88	218.67	221.28
2024	270.73	278.92	274.83	289.03	315.02	302.03	222.23	231.37	226.8
2025	270.24	269.77	270.01	301.44	310.58	306.01	203.42	204.68	204.05
2026	306.08	296.97	301.53	322.7	336.17	329.44	226.21	208.29	217.25
2027	288.32	283.61	285.97	307	316.5	311.75	221.71	224.79	223.25
2028	267.83	275.11	271.47	310.6	318.38	314.49	200.42	252.36	226.39
2029	267.11	266.97	267.04	291.24	318.59	304.92	230.16	275.82	252.99
2030	283.19	292.01	287.6	304.77	342.51	323.64	243.21	256.01	249.61
2031	258.44	267.52	262.98	298	310.49	304.25	234.15	244.14	239.15
2032	290.15	305.6	297.87	318.95	340.41	329.68	237.9	306.95	272.42
2033	259.35	278.36	268.86	303.18	325.44	314.31	238.37	291.62	264.99
2034	271.14	299.28	285.21	313.53	343.08	328.3	246.95	299.26	273.11
2035	266.89	285.82	276.36	291.85	334.87	313.36	239.54	323.41	281.47

Fig. 10. Average of ET<sub>c</sub> values during the historical, future periods, and their expected percentages for the three regions.

changes on wheat evapotranspiration (ET<sub>c</sub>) using deep neural networks (DNN) method. Three Egyptian governorates were selected in Nile Delta namely Ad Daqahliyah, Kafr ash Shaykh, and Ash Sharqiyah. The monthly data of minimum temperature ( $T_{\min}$ ), maximum temperature ( $T_{\max}$ ), and solar radiation (SR) were obtained from open access data over the period from 1970 to 2000 and from 2000–2017 for calibration and validation. In addition, the climate weather data were collected from two Representative Concentration Pathways during 2022–2035. After generating ET<sub>c</sub> by Hargreaves method with historical and future weather data, the historical data were entered as inputs for valuing the outputs of the generated DNN model. The results showed a high correlation between actual-predicted ET<sub>c</sub> values for calibration and validation periods over the three study regions. After generating good results from the DNN model through the historical period, the future dataset was incorporated to predict the future ET<sub>c</sub>. The model findings indicated that Kafr Ash Shaykh will achieve the first rank for recording a high increased by 11.31 % then Ad Daqahliyah with an increased by 1.38 %. On the other hand, the expected results stated that Ash Sharqiyah region would decrease by 15.09 % compared to the historical dataset. These created DNN models produced satisfactory outputs with high accuracy for the three regions. Therefore, these models will help the water managers-planners and decision-

makers for long term water sustainability. This study is essential as an important step in supporting agricultural water management strategies, for crop-water modeling. Our recommendations can be used on large scale in all Nile Delta governorates as a rapid, robust and reliable technique for modeling ET<sub>c</sub> using limited meteorological data and simple method. In the future, the proposed model can be applied to other economic crops, such as rice and maize, for modeling ET<sub>c</sub> to achieve sustainable agricultural water management.

#### Author contributions

Ahmed Elbeltagi and Jinsong Deng had the original idea for the study and all coauthors conceived and designed the study. Ahmed Elbeltagi analyzed data and wrote the paper, which was revised by Jinsong Deng; and all authors read and approved the final manuscript.

#### Declaration of Competing Interest

The authors declare no conflict of interest

## Acknowledgements

This work was supported by Zhejiang Provincial Natural Science Foundation of China [grant number LY18G030006]. Cordial thanks are extended to the editor and seven anonymous reviewers for their helpful feedback.

## References

- Abatzoglou, J.T., Dobrowski, S.Z., Parks, S.A., Hegewisch, K.C., 2018. TerraClimate, a high-resolution global dataset of monthly climate and climatic water balance from 1958–2015. *Sci. Data* 5, 1–12. <https://doi.org/10.1038/sdata.2017.191>.
- Abdelmaged, K., Xu-hong, C., De-mei, W., Yan-jie, W., Yu-shuang, Y., 2019. Evolution of varieties and development of production technology in Egypt wheat: a review. *J. Integr. Agric.* 18, 483–495. [https://doi.org/10.1016/S2095-3119\(18\)62053-2](https://doi.org/10.1016/S2095-3119(18)62053-2).
- Agrometeorological Centre of Excellence, 2020. n.d. Agricultural Statistics Index. URL <http://www.gov.mb.ca/agriculture/climate> (Accessed 12.28.18).
- Aguilar, C., Polo, M.J., Dynamics, F., 2011. Generating reference evapotranspiration surfaces from the Hargreaves equation at watershed scale. *Hydrol. Earth Syst. Sci. Discuss.* 15, 2495–2508. <https://doi.org/10.5194/hess-15-2495-2011>.
- Aladenola, O., Madramootoo, C., 2010. Development of a model for estimating current and future irrigation water demand in Canada. *XVIIIth World Congr. Int. Comm. Agric. Biosyst. Eng.* 1–10.
- Allen, R.G., Pereira, L.S., Raes, D., Smith, M., 1998. FAO irrigation and drainage paper. *Fao* 300, 326. <https://doi.org/10.1016/j.eja.2010.12.001>.
- Almorox, J., Quej, V.H., Martí, P., 2015. Global performance ranking of temperature-based approaches for evapotranspiration estimation considering Köppen climate classes. *J. Hydrol.* 528, 514–522. <https://doi.org/10.1016/j.jhydrol.2015.06.057>.
- Anselin, L., Syabri, I., Kho, Y., 2006. GeoDa: an introduction to spatial data analysis. *Geogr. Anal.* 38, 5–22 ISSN 0016-7363 (the Ohio State Univ.
- Anwer, S., Almaraf, D., Hikmat, E.F., 2016. Predicting the crop coefficient values for maize in Iraq. *Eng. & Tech. Journal* 34, 284–294.
- Awal, R., Habibi, H., Fares, A., Deb, S., 2020. Regional Studies estimating reference crop evapotranspiration under limited climate data in West Texas. *J. Hydrol. Reg. Stud.* 28, 100677. <https://doi.org/10.1016/j.ejrh.2020.100677>.
- Barger, G.L., 1969. Total growing degree days. *Wkly. Weather Crop Bull.* 56, 10.
- Butler, A.P., Neale, C.M.U., Raes, D., Steduto, P., Fereres, E., Foster, T., Brozovi, N., Hsiao, T.C., 2017. AquaCrop-OS: an open source version of FAO's crop water productivity model. *Agric. Water Manag.* 181, 18–22. <https://doi.org/10.1016/j.agwat.2016.11.015>.
- Chen, Y., Marek, G.W., Marek, T.H., Moorhead, J.E., Heflin, K.R., Brauer, D.K., Gowda, P.H., Srinivasan, R., 2019. Simulating the impacts of climate change on hydrology and crop production in the Northern High Plains of Texas using an improved SWAT model. *Agric. Water Manag.* 221, 13–24. <https://doi.org/10.1016/j.agwat.2019.04.021>.
- Chen, Z., D. S.S.P., Wang, Y., Wang, Q., Zhang, X., 2020. Temporal convolution-network-based models for modeling maize evapotranspiration under mulched drip irrigation. *Comput. Electron. Agric.* 169, 105206. <https://doi.org/10.1016/j.compag.2019.105206>.
- Chia, M.Y., Huang, Y.F., Koo, C.H., Fung, K.F., 2020. Recent advances in evapotranspiration estimation using artificial intelligence approaches with a focus on hybridization techniques — a review. *Agronomy* 10, 1–33.
- Dadaşer-celik, F., Cengiz, E., Guzel, O., 2016. Trends in reference evapotranspiration in Turkey: 1975–2006. *Int. J. Climatol.* 36, 1733–1743. <https://doi.org/10.1002/joc.4455>.
- Elbeltagi, A., Deng, J., Wang, K., Hong, Y., 2020a. Crop Water footprint estimation and modeling using an artificial neural network approach in the Nile Delta. *Egypt. Agric. Water Manag.* 235, 106080. <https://doi.org/10.1016/j.agwat.2020.106080>.
- Elbeltagi, A., Zhang, L., Deng, J., Juma, A., Wang, K., 2020b. Modeling monthly crop coefficients of maize based on limited meteorological data: a case study in Nile Delta, Egypt. *Comput. Electron. Agric.* 173, 105368. <https://doi.org/10.1016/j.compag.2020.105368>.
- Esparafor, M., Lorite, I.J., Gavilán, P., Berengena, J., 2011. An analysis of the tendency of reference evapotranspiration estimates and other climate variables during the last 45 years in Southern Spain. *Agric. Water Manag.* 98, 1045–1061. <https://doi.org/10.1016/j.agwat.2011.01.015>.
- Espejo-García, B., Lopez-pellicer, F.J., Lacasta, J., Piedra, R., Zarazaga-soria, F.J., 2019. End-to-end sequence labeling via deep learning for automatic extraction of agricultural regulations. *Comput. Electron. Agric.* 162, 106–111. <https://doi.org/10.1016/j.compag.2019.03.027>.
- Everton, J., Santos, O., França, F., Filgueiras, R., Henrique, G., Heriberto, A., Teixeira, D.C., Charles, F., Chohaku, G., 2020. Performance of SAFER evapotranspiration using missing meteorological data. *Agric. Water Manag.* 233, 106076. <https://doi.org/10.1016/j.agwat.2020.106076>.
- Falamarzi, Y., Palizdan, N., Feng, Y., Shui, T., 2014. Estimating evapotranspiration from temperature and wind speed data using artificial and wavelet neural networks (WNNs). *Agric. Water Manag.* 140, 26–36. <https://doi.org/10.1016/j.agwat.2014.03.014>.
- Fan, H., Jiang, M., Xu, L., Zhu, H., Cheng, J., 2020. Comparison of long short term memory networks and the hydrological model in runoff simulation. *Water (Switzerland)* 2, 1–15. <https://doi.org/10.3390/w12010175>.
- FAO, 2000. Irrigation and Drainage Paper | Crop Evapotranspiration. 326. [https://doi.org/10.1016/S0141-1187\(05\)80058-6](https://doi.org/10.1016/S0141-1187(05)80058-6).
- FAO, 2011. Agricultural Data FAOSTAT. Food and Agriculture Organization of the United Nations, Rome, Italy.
- Farg, E., Arafat, S.M., Abd El-Wahed, M.S., El-Gindy, A.M., 2012. Estimation of evapotranspiration ETc and crop coefficient Kc of wheat, in south nile Delta of Egypt using integrated FAO-56 approach and remote sensing data. *Egypt. J. Remote Sens. Sp. Sci.* 15, 83–89. <https://doi.org/10.1016/j.ejrs.2012.02.001>.
- Feng, Y., Jia, Y., Cui, N., Zhao, L., Li, C., Gong, D., 2017. Calibration of Hargreaves model for reference evapotranspiration estimation in Sichuan basin of southwest China. *Agric. Water Manag.* 181, 1–9. <https://doi.org/10.1016/j.agwat.2016.11.010>.
- Ferreira, L.B., França, F., 2020. New approach to estimate daily reference evapotranspiration based on hourly temperature and relative humidity using machine learning and deep learning. *Agric. Water Manag.* 234, 106113. <https://doi.org/10.1016/j.agwat.2020.106113>.
- Fooladmand, H.R., Zandilak, H., 2008. Comparison of different types of Hargreaves equation for estimating monthly evapotranspiration in the south of Iran. *Arch. Agron. Soil Sci.* 54, 321–330. <https://doi.org/10.1080/03650340701793603>.
- Gavila, P., Joaquin, B., Allen, R.G., 2007. Measuring versus estimating net radiation and soil heat flux: impact on Penman – monteith reference ET estimates in semiarid regions. *Agric. Water Manag.* 89, 275–286. <https://doi.org/10.1016/j.agwat.2007.01.014>.
- Gocic, M., Trajkovic, S., Shamshirband, S., Motamed, S., 2015. Determination of the most influential weather parameters on reference evapotranspiration by adaptive neuro-fuzzy methodology. *Comput. Electron. Agric.* 114, 277–284. <https://doi.org/10.1016/j.compag.2015.04.012>.
- Gonzalez, R.T., Subathra, M.S.P., Manoj, N., Verrastro, S., George, S.T., 2020. Modelling the daily reference evapotranspiration in semi-arid region of South India: a case study comparing ANFIS and empirical models. *Inf. Process. Agric.* <https://doi.org/10.1016/j.inpa.2020.02.003>.
- Gutowski, W., Giorgi, F., Timbal, B., Frigon, A., Jacob, D., Kang, H., Raghavan, K., Lee, B., Lennard, C., Nikulin, G., Rourke, E.O., Rixen, M., 2016. WCRP COordinated regional downscaling EXperiment (CORDEX): a diagnostic MIP for CMIP6. *Geosci. Model. Dev. Discuss.* 9, 4087–4095. <https://doi.org/10.5194/gmd-9-4087-2016>.
- Hargreaves, G.H., Allen, R.G., 2003. History and evaluation of hargreaves evapotranspiration equation. *J. Irrig. Drain. Eng.* 129, 53–63. [https://doi.org/10.1016/ASCE0733-9437\(2003\)129:1\(53\)](https://doi.org/10.1016/ASCE0733-9437(2003)129:1(53)).
- Hassan, A., Aitazaz, A., Farhat, A., Bishnu, A., Travis, E., 2020. Groundwater estimation from major physical hydrology components using artificial neural networks and deep learning. *Water (Switzerland)* 12, 1–18.
- Hobbins, M., 2016. The variability of ASCE Standardized reference evapotranspiration: a rigorous, CONUS-wide decomposition and attribution. *Am. Soc. Agric. Biol. Eng.* 59, 561–576. <https://doi.org/10.13031/trans.59.10975>.
- Huang, Q., Tang, C., Chen, Z., Li, S., Li, J., 2020. Numerical simulation of evapotranspiration with limited data in the Pearl River Basin. *Mater. Sci. Forum* 980, 512–524. <https://doi.org/10.4028/www.scientific.net/MSF.980.512>.
- Irmak, S., Kabenge, I., Skaggs, K.E., Muttiibwa, D., 2012. Trend and magnitude of changes in climate variables and reference evapotranspiration over 116-yr period in the Platte River Basin, central Nebraska – USA. *J. Hydrol.* 420–421, 228–244. <https://doi.org/10.1016/j.jhydrol.2011.12.006>.
- Jensen, M.E., Allen, R.G., 2016. Evaporation, evapotranspiration, and irrigation water requirements. *Am. Soc. Civil Eng.*
- Jeong, E., Choi, J.A., Young, J., 2010. Estimation of future reference crop evapotranspiration using artificial neural networks. *J. Korean Soc. Agric. Eng.* 52, 1–9. <https://doi.org/10.5389/KSAE.2010.52.5.001>.
- Jung, S., McDonald, K., 2011. Visual gene developer: a fully programmable bioinformatics software for synthetic gene optimization. *BMC Bioinforma* 2011 <http://www.biomedcentral.com/1471-2105/12/340> 1–13.
- Kang, H., Chen, C., 2020. Fast implementation of real-time fruit detection in apple orchards using deep learning. *Comput. Electron. Agric.* 168, 105108. <https://doi.org/10.1016/j.compag.2019.105108>.
- Khoshravesh, M., Ali, M., Sefidkouhi, G., Valipour, M., 2017. Estimation of reference evapotranspiration using multivariate fractional polynomial, Bayesian regression, and robust regression models in three arid environments. *Appl. Water Sci.* 7, 1911–1922. <https://doi.org/10.1007/s13201-015-0368-x>.
- Kisi, O., 2016. Modeling reference evapotranspiration using three different heuristic regression approaches. *Agric. Water Manag.* 169, 162–172. <https://doi.org/10.1016/j.agwat.2016.02.026>.
- Kisi, O., Alizamir, M., 2018. Modelling reference evapotranspiration using a new wavelet conjunction heuristic method: wavelet extreme learning machine vs wavelet neural networks. *Agric. For. Meteorol.* 263, 41–48. <https://doi.org/10.1016/j.agrformet.2018.08.007>.
- Kisi, O., Sanikhani, H., Zounemat-kermani, M., Niazi, F., 2015. Long-term monthly evapotranspiration modeling by several data-driven methods without climatic data. *Comput. Electron. Agric.* 115, 66–77. <https://doi.org/10.1016/j.compag.2015.04.015>.
- Kobayashi, S., Ota, Y., Harda, Y., Ebata, A., Moriya, M., Onoda, H., Onogi, K., Kamahori, H., Kobayashi, C., Endo, H., Miyaoka, K., Takahashi, K., 2015. The JRA-55 reanalysis: general specifications and basic characteristics. *J. Meteorol. Soc. Japan. Ser. II* 93, 5–48. <https://doi.org/10.2151/jms.2015-001>.
- Kounalakis, T., Triantafyllidis, G.A., Nalpantidis, L., 2019. Deep learning-based visual recognition of rumex for robotic precision farming. *Comput. Electron. Agric.* 165, 104973. <https://doi.org/10.1016/j.compag.2019.104973>.
- Lee, S.H., Goéau, H., Bonnet, P., Joly, A., 2020. New perspectives on plant disease characterization based on deep learning. *Comput. Electron. Agric.* 170, 105220. <https://doi.org/10.1016/j.compag.2020.105220>.
- Li, Z., Zheng, F., Liu, W., 2012. Spatiotemporal characteristics of reference evapotranspiration during 1961–2009 and its projected changes during 2011–2099 on the

- Loess Plateau of China. *Agric. For. Meteorol.* 154–155, 147–155. <https://doi.org/10.1016/j.agrformet.2011.10.019>.
- Li, J., Zhu, T., Mao, X., Adeloye, A.J., 2016. Modeling crop water consumption and water productivity in the middle reaches of Heihe River Basin. *Modeling crop water consumption and water productivity in the middle reaches of Heihe River Basin. Comput. Electron. Agric.* 123, 242–255. <https://doi.org/10.1016/j.compag.2016.02.021>.
- Luhunga, P.M., Kijazi, A.L., Chang, L., Kondowe, A., 2018. Climate change projections for Tanzania Based on high-resolution regional climate models from the coordinated regional climate downscaling experiment (CORDEX)-Africa. *Front. Environ. Sci.* 6, 1–20. <https://doi.org/10.3389/fenvs.2018.00122>.
- Ma, J., Du, K., Zheng, F., Zhang, L., Gong, Z., Sun, Z., 2018. A recognition method for cucumber diseases using leaf symptom images based on deep convolutional neural network. *Comput. Electron. Agric.* 154, 18–24. <https://doi.org/10.1016/j.compag.2018.08.048>.
- Majeed, Y., Zhang, J., Zhang, X., Fu, L., Karkee, M., Zhang, Q., 2020. Deep learning based segmentation for automated training of apple trees on trellis wires. *Comput. Electron. Agric.* 170, 105277. <https://doi.org/10.1016/j.compag.2020.105277>.
- Malik, A., Kumar, A., Ghorbani, M.A., Kashani, M.H., Kisi, O., Kim, S., 2019. The viability of co-active fuzzy inference system model for monthly reference evapotranspiration estimation: case study of Uttarakhand State. *Hydrol. Res.* 23, 1–22. <https://doi.org/10.2166/nh.2019.059>.
- Maroufpoor, S., Maroufpoor, E., Bozorg-haddad, O., Shiri, J., 2019a. Soil moisture simulation using hybrid artificial intelligent model: hybridization of adaptive neuro fuzzy inference system with grey wolf optimizer algorithm. *J. Hydrol.* 575, 544–556. <https://doi.org/10.1016/j.jhydrol.2019.05.045>.
- Maroufpoor, S., Shiri, J., Maroufpoor, E., 2019b. Modeling the sprinkler water distribution uniformity by data-driven methods based on effective variables. *Agric. Water Manag.* 215, 63–73. <https://doi.org/10.1016/j.agwat.2019.01.008>.
- Maroufpoor, S., Bozorg-haddad, O., Maroufpoor, E., 2020. Reference evapotranspiration estimating based on optimal input combination and hybrid artificial intelligent model: hybridization of artificial neural network with grey wolf optimizer algorithm. *J. Hydrol.* 125060. <https://doi.org/10.1016/j.jhydrol.2020.125060>.
- Maselli, F., Chiesi, M., Angeli, L., Fibbi, L., Rapi, B., Romani, M., Sabatini, F., Battista, P., 2020. An improved NDVI-based method to predict actual evapotranspiration of irrigated grasses and crops. *Agric. Water Manag.* 233, 106077. <https://doi.org/10.1016/j.agwat.2020.106077>.
- Masud, M., Mcallister, T., Cordeiro, M.R.C., Faramarzi, M., 2018. Modeling future water footprint of barley production in Alberta, Canada: implications for water use and yields to 2064. *Sci. Total Environ.* 616–617, 208–222. <https://doi.org/10.1016/j.scitotenv.2017.11.004>.
- Mehdi, B., Vienna, L.S., 2010. Estimation of future crop water requirements for 2020 and 2050, using CROPWAT. *Conf. Pap. Authorized Licensed Use Limited to: McGill Univers.* <https://doi.org/10.1109/EICCCC.2006.277194>.
- Mehdizadeh, S., 2018. Estimation of daily reference evapotranspiration (ET<sub>0</sub>) using artificial intelligence methods: offering a new approach for lagged ET<sub>0</sub> data-based modeling. *J. Hydrol.* <https://doi.org/10.1016/j.jhydrol.2018.02.060>.
- Mehdizadeh, S., Behmanesh, J., Khalili, K., 2017. Using MARS, SVM, GEP and empirical equations for estimation of monthly mean reference evapotranspiration. *Comput. Electron. Agric.* 139, 103–114. <https://doi.org/10.1016/j.compag.2017.05.002>.
- Mehra, M., Saxena, S., Sankaranarayanan, S., Tom, R.J., Veeramanikandan, M., 2018. IoT based hydroponics system using deep neural networks. *Comput. Electron. Agric.* 155, 473–486. <https://doi.org/10.1016/j.compag.2018.10.015>.
- Mohammadi, B., Mehdizadeh, S., 2020. Modeling daily reference evapotranspiration via a novel approach based on support vector regression coupled with whale optimization algorithm. *Agric. Water Manag.* <https://doi.org/10.1016/j.agwat.2020.106145>.
- Motamed, S., Shamshirband, S., Petkovic, D., Ch, S., Hashim, R., Arif, M., 2015. Soft computing approaches for forecasting reference evapotranspiration. *Comput. Electron. Agric.* 113, 164–173. <https://doi.org/10.1016/j.compag.2015.02.010>.
- Mulovhedzi, N.E., Araya, N.A., Mengistu, M.G., Fessehazion, M.K., Plooy, C.P., Araya, H.T., Laan, M..Van Der, 2020. Estimating evapotranspiration and determining crop coefficients of irrigated sweet potato (*Ipomoea batatas*) grown in a semi-arid climate. *Agric. Water Manag.* 233, 106099. <https://doi.org/10.1016/j.agwat.2020.106099>.
- Onwuegbunam, N.E., Onwuegbunam, D., Dare, A., 2020. Estimation and comparison of reference evapotranspiration within kaduna central district, Nigeria, using four different methods. *Niger. J. Technol.* 39, 306–314.
- Patel, J., Patel, H., Bhatt, C., 2014. Generalized calibration of the hargreaves equation for evapotranspiration under different climate conditions. *Soil Water Res.* 9, 83–89.
- Pereira, L.S., Allen, R.G., Smith, M., Raes, D., 2014. Crop evapotranspiration estimation with FAO56: past and future. *Agric. Water Manag.* 1–16. <https://doi.org/10.1016/j.agwat.2014.07.031>.
- Picon, A., Alvarez-gila, A., Seitz, M., Ortiz-barredo, A., Echazarra, J., Johannes, A., 2018. Deep convolutional neural networks for mobile capture device-based crop disease classification in the wild. *Comput. Electron. Agric.* 0–1. <https://doi.org/10.1016/j.compag.2018.04.002>.
- Pôças, I., Paço, T.A., Paredes, P., Cunha, M., Pereira, L.S., 2015. Estimation of actual crop coefficients using remotely sensed vegetation indices and soil water balance modelled data. *Remote Sens.* 7, 2373–2400. <https://doi.org/10.3390/rs70302373>.
- Raziee, T., Pereira, L.S., 2013. Estimation of ET<sub>0</sub> with Hargreaves – samani and FAO-PM temperature methods for a wide range of climates in Iran. *Agric. Water Manag.* 121, 1–18. <https://doi.org/10.1016/j.agwat.2012.12.019>.
- Saggi, M.K., Jain, S., 2019a. Application of fuzzy-genetic and regularization random forest (FG-RRF): estimation of crop evapotranspiration (ET<sub>c</sub>) for maize and wheat crops. *Agric. Water Manag.* <https://doi.org/10.1016/j.agwat.2019.105907>.
- Saggi, M.K., Jain, S., 2019b. Reference evapotranspiration estimation and modeling of the Punjab Northern India using deep learning. *Comput. Electron. Agric.* 156, 387–398. <https://doi.org/10.1016/j.compag.2018.11.031>.
- Sammis, T.W., Mapel, C.L., Lugg, D.G., Lansford, R.R., McGuckin, J.T., 1985. Evapotranspiration crop coefficients predicted using growing-degree days. *Trans. ASAE* 28, 773–780.
- Sayed, H., Abdelaal, A., Thilmany, D., 2019. Grains production prospects and long run food security in Egypt. *Sustainability* 11, 1–17.
- Yamaç, S.S., Todorovic, M., 2020. Estimation of daily potato crop evapotranspiration using three different machine learning algorithms and four scenarios of available meteorological data. *Agric. Water Manag.* 228, 105875.
- Seyedzadeh, A., Maroufpoor, S., Maroufpoor, E., Shiri, J., 2019. Artificial intelligence approach to estimate discharge of drip tape irrigation based on temperature and pressure. *Agric. Water Manag.*, 105905. <https://doi.org/10.1016/j.agwat.2019.105905>.
- Shalaby, A., 2012. Assessment of urban sprawl impact on the agricultural land in the Nile Delta of Egypt using remote sensing and digital soil map. *Int. J. Environ. Sci.* 1, 253–262.
- Shalaby, A., Tateishi, R., 2007. Remote sensing and GIS for mapping and monitoring land cover and land-use changes in the Northwestern coastal zone of Egypt. *Appl. Geogr.* 27, 28–41. <https://doi.org/10.1016/j.apgeog.2006.09.004>.
- Surendran, U., Sushanth, C.M., Mammen, G., Joseph, E.J., 2015. Modelling the crop water requirement using FAO-CROPWAT and assessment of water resources for sustainable water resource management : a case study in Palakkad district of humid tropical Kerala, India. *Aquat. Procedia* 4, 1211–1219. <https://doi.org/10.1016/j.aqpro.2015.02.154>.
- Tabari, H., Grísmér, M.E., Trajkovic, S., 2013. Comparative analysis of 31 reference evapotranspiration methods under humid conditions. *Irrig. Sci.* 31, 107–117. <https://doi.org/10.1007/s00271-011-0295-z>.
- Tao, X., Chen, H., Xu, C., Hou, Y., Jie, M., 2015. Analysis and prediction of reference evapotranspiration with climate change in Xiangjiang River Basin, China. *Water Sci. Eng.* 8, 273–281. <https://doi.org/10.1016/j.wse.2015.11.002>.
- Taylor, K., Stouffer, R., Meehl, G., 2012. An Overview of CMIP5 and the experiment design. *Am. Meteorol. Soc.* 3, 485–498. <https://doi.org/10.1175/BAMS-D-11-00094.1>.
- Thenmozhi, K., Reddy, U.S., 2019. Crop pest classification based on deep convolutional neural network and transfer learning. *Comput. Electron. Agric.* 164, 104906. <https://doi.org/10.1016/j.compag.2019.104906>.
- Tikhamarine, Y., Malik, A., Kumar, A., Souag-gamane, D., Kisi, O., 2019. Estimation of monthly reference evapotranspiration using novel hybrid machine learning approaches. *Hydrol. Sci. J. Des Sci. Hydrol.* 0, 1. <https://doi.org/10.1080/02626667.2019.1678750>.
- Tikhamarine, Y., Malik, A., Souag-gamane, D., Kisi, O., 2020. Artificial intelligence models versus empirical equations for modeling monthly reference evapotranspiration. *Environ. Sci. Pollut. Res.*
- Vinayaka, S., Suzanna, L., 2020. Flood prediction and uncertainty estimation using deep learning. *Water (Switzerland)* 12, 1–16.
- Wang, J., Ma, Y., Zhang, L., Gao, R.X., Wu, D., 2018. Deep learning for smart manufacturing : methods and applications. *Int. J. Ind. Manuf. Syst.* 1–13. <https://doi.org/10.1016/j.jimsy.2018.01.003>.
- Wang, S., Lian, J., Peng, Y., Hu, B., Chen, H., 2019. Generalized reference evapotranspiration models with limited climatic data based on random forest and gene expression programming in Guangxi, China. *Agric. Water Manag.* 221, 220–230. <https://doi.org/10.1016/j.agwat.2019.03.027>.
- Xiao, D., Bai, H., Liu, D.L., 2018. Impact of future climate change on wheat production: a simulated case for China's wheat system. *Sustain.* 10, 1–15. <https://doi.org/10.3390/su10041277>.
- Zhang, Y., Cai, J., Xiao, D., Li, Z., Xiong, B., 2019. Real-time sow behavior detection based on deep learning. *Comput. Electron. Agric.* 163, 104884. <https://doi.org/10.1016/j.compag.2019.104884>.